IN-1110
December 1967

RADIATIVE AND CONVECTIVE HEAT TRANSFER WITHIN VERTICAL ANNULAR SPACES OPEN AT THE ENDS

J. C. Petrie, B. R. Dickey, and B. M. Legler

IDAHO NUCLEAR CORPORATION
NATIONAL REACTOR TESTING STATION
IDAHO FALLS, IDAHO

U. S. ATOMIC ENERGY COMMISSION

DISCLAIMER

Printed in the United States of America
Available from
Clearinghouse for Federal Scientific and Technical Information
National Bureau of Standards, U. S. Department of Commerce
Springfield, Virginia 22151
Price: Printed Copy $3.00; Microfiche $0.65

LEGAL NOTICE

IN-1110
Issued: December 1967
[Waste Disposal and Processing]
TID-4500

RADIATIVE AND CONVECTIVE HEAT TRANSFER WITHIN VERTICAL ANNULAR SPACES OPEN AT THE ENDS

J. C. Petrie
B. R. Dickey
B. M. Legler

IDAHO NUCLEAR CORPORATION

A JOINTLY OWNED SUBSIDIARY OF
AEROJET GENERAL CORPORATION
ALLIED CHEMICAL CORPORATION

U. S. Atomic Energy Commission Research and Development Report
Issued Under Contract AT(10-1)-1230
Idaho Operations Office

ABSTRACT

Convective and radiative heat transfer within a vertical cylindrical annulus open at the ends has been investigated. Data for natural convective heat transfer from the inner cylinder are compared with data for natural convective heat transfer from isolated surfaces. The rate of heat transfer across the annulus by conduction and convection is calculated by means of a pseudo-effective thermal conductivity, the resulting values being up to 1.8 times the effective conductivity for a completely enclosed annulus. Radiative heat transfer from the inner to the outer cylinder was calculated using a digital computer program based on the absorption factor method of Gebhart.

CONTENTS

FIGURES

TABLES

TABLES (continued)

SUMMARY

Heat transfer within vertical cylindrical annuli has been correlated both in terms of the Nusselt number versus the Rayleigh number and in terms of an effective thermal conductivity versus the Grashof number. Results from this study include: (1) experimental data on the radiative and convective heat transfer within a vertical annulus open at the ends, and (2) correlation of the resistance to heat flow within the annulus in terms of an effective thermal conductivity.

It has been shown that existing correlations for natural convective heat transfer from isolated vertical surfaces can be applied to convective transfer within annuli open at the ends. However, the temperatures of both the inner cylinder and the air within the annulus are increased because of inward radiation from the outer cylinder.

Pseudo-effective thermal conductivities for the vertical annulus open at the ends are 1.2 - 1.8 times the effective conductivities for a completely enclosed annulus. Convective motion for the open-ended annulus is negligible below a Rayleigh number of approximately 100, whereas convection is negligible below a Rayleigh number of 1700 for a completely enclosed annulus.

I. INTRODUCTION

The Waste Calcining Facility at the Idaho Chemical Processing Plant (ICPP) converts aqueous radioactive wastes to free-flowing granular solids by a fluidized bed calcining process[1]. The granular solids, containing the bulk of the fission products from the original liquid waste, are stored within cylindrical bins in an underground vault.

Heat generated by radioactive decay of fission products within the stored solids must be removed at temperatures where: (1) the structural integrity of the storage vessel is not threatened, and (2) fission product volatilization is not possible. Removal of heat solely by conduction to the surrounding soil may result in excessive temperatures within the stored wastes[2]; thus, additional means of heat removal are provided. The heat is currently removed by natural convection from the bins to the air in the vault followed by a combination of convection and radiation to the vault wall. The major portion of the heat is ultimately removed by conduction through the soil surrounding the vault wall.

This study was undertaken to determine the rate of heat flow within an air gap, separating a heated vertical cylinder from a surrounding shroud, in a system which geometrically simulates a portion of one of the storage bins containing solidified waste at the ICPP[3]. A determination of the quantity of heat transferred by radiation and the combined mechanisms of convection and conduction is necessary in understanding the overall energy transport. A generalized correlation is needed to provide a means of predicting the resistance to heat flow within an air-filled annulus open at both ends.

Heat transfer across an enclosed fluid-filled annulus has been extensively studied and reported in the literature[4,5,6]. The insulating effect of enclosed vertical air layers is well known (brick walls and double-glass windows), and the phenomenon of natural circulation induced by temperature gradients within an enclosed space has been thoroughly investigated. However, no reports of studies of heat transfer by natural convection within an annulus open at both ends have been found in the literature.

Data for heat transfer within enclosed fluid-filled spaces have been correlated by two different formulae, one presented by Jacob[4] and the other by Grober, Erk, and Grigull[5]. Both correlations employ the ratio of an effective thermal conductivity to the normal conductivity (based on arithmetic mean temperature) of the fluid as a measure of the extent of convective motion in the annulus. Jacob's correlation is:

$$k_e/k = C\,(N'_{Gr})^n\,(L/S)^{-1/9} \qquad (1)$$

where:

k_e = effective thermal conductivity across the annular space, Btu/hr-ft-^oF

k = thermal conductivity of the fluid based on arithmetic average temperature, Btu/hr-ft-^oF

$(N'_{Gr} = \frac{g\beta\Delta TS^3}{\mu^2})$ = Grashof number based on annular spacing, dimensionless

L/S = ratio of height to annular separation, dimensionless

C,n = constants depending on flow characteristics, dimensionless.

In the laminar range of Grashof numbers between 2×10^4 and 2×10^5, $C = 0.18$ and $n = 1/4$. In the turbulent range of Grashof numbers between 2×10^5 and 1.1×10^7, $C = 0.065$ and $n = 1/3$. The exponents of 1/4 and 1/3 are conventional for laminar and turbulent flow, respectively.

Data for heat transfer within both vertical and horizontal annular spaces (closed at the ends) separated by constant temperature surfaces are presented by Grober, Erk, and Grigull[5]. The data are correlated by:

$$k_e/k = K\,(N'_{Ra})^n \qquad (2)$$

where:

k, k_e = as previously defined

$(N'_{Ra} = N'_{Gr}\,N_{Pr})$ = Rayleigh number based on annular separation, dimensionless

K,n = constants, dimensionless

The values of K and n are dependent on the Rayleigh number. For Rayleigh numbers between 6×10^3 and 10^6, $K = 0.11$ and $n = 0.29$; for Rayleigh numbers between 10^6 and 10^8, $K = 0.40$ and $n = 0.20$. The values of n do not agree with the familiar values for laminar and turbulent flow.

Values of k_e in the above correlations can be determined from:

$$Q_c = \frac{k_e A_m}{S}(T_1 - T_2) \tag{3}$$

where:

Q_c = convective heat transfer rate, Btu/hr

S = annular spacing, ft

A_m = log mean area of the annular space, ft^2

T_1 = surface temperature of inner cylinder, ^oF

T_2 = surface temperature of outer cylinder, ^oF.

Ostrach derived dimensionless temperature and velocity profiles for natural convective heat transfer from an isolated vertical plate[5]. At some distance from the heated surface, depending on the Prandtl number of the fluid, the velocity and temperature profiles become essentially flat. For fluids having a Prandtl number of 0.72 (air at normal temperatures) the profiles flatten at a dimensionless distance, η, of about 4. The definition of η is:

$$\eta = (Y/X)^4 \frac{N_{Gr,X}}{4} \tag{4}$$

where:

η = dimensionless width of velocity and temperature profile

Y = thickness of boundary layer, consistent units

X = vertical height of plate, consistent units

$N_{Gr,X}$ = Grashof number based on vertical height, X.

Because of the relatively large diameter of the heated cylinder used in this study, the boundary layer theory as proposed by Ostrach for flat surfaces can be applied with little error. At a Grashof number of 10^8 and a plate height of 27 inches (approximately that used in this study) the maximum boundary layer thickness is about an inch. The boundary layer thickness increases along the height of the surface, attaining the maximum thickness at the top of the cylinder.

Ideally, there should be no effect of a nearby surface on natural convection from a given surface unless the boundary layers interact. Therefore, correlations using the conventional Nusselt and Rayleigh numbers for natural convective heat transfer should apply only until the annular separation is less than two boundary layer thicknesses.

II. EXPERIMENTAL PROCEDURE AND DESCRIPTION OF EQUIPMENT

The equipment used in this study was fabricated to simulate geometrically a portion of one of the actual solids storage bins. Heat was supplied to an inner cylinder and was dissipated by the mechanisms of radiation, conduction, and convection to the annulus and the surrounding shroud. Temperatures of the source, shroud, and the inlet and outlet air were measured to permit calculation of the heat transfer rates by the various mechanisms. The flow of air through the annulus, measured by a hot-wire anemometer, was used in a calculation of the emissivity of the stainless steel surfaces. Although the geometry of the apparatus simulates a specific unit, the results have been correlated in a manner useful in predicting the resistance to heat flow within an air-filled annulus.

Test Equipment and Procedure

A cut-away view of the test equipment is shown in Figure 1. Two electrical resistance heaters, butted together axially, supplied heat to the source. Heat was transferred by conduction through the solid aluminum-filled center to the walls of the eight-inch-diameter pipe surrounding the heat source; a constant heat flux at the surface of the inner cylinder resulted from insulating the ends of the source. Heat was transferred from the surface of the source by radiation and convection to the surroundings and by natural convection to the air within the space. Buoyancy of the heated air within the annular gap caused a positive flow of air upward through the open ends of the vertical annulus. The apparatus was designed to permit placement of a concentric shroud around the heat source. Shrouds of various diameters were constructed to provide the several annular spacings used in the study. Small spacers were used to separate the heat source from the air inlet pipe at the bottom of the shell (Figure 1).

The power to the source was measured by a wattmeter installed in the electrical line to the parallel-wired resistance heaters. The electrical power was controlled manually by a powerstat connected to a 220-volt power supply.

A cross-sectional view of the heat source is shown in Figure 2. Uniform contact resistance between the heaters and the aluminum filler was insured by close-tolerance machining and forced fitting. The shell of the heat source was fabricated by welding an eight-inch cap to an eight-inch Schedule 40 pipe, both of Type 304 stainless steel. The inside surface was machined to a slight taper (0.004 inch in the 27-inch length) to match the aluminum metal filler by an

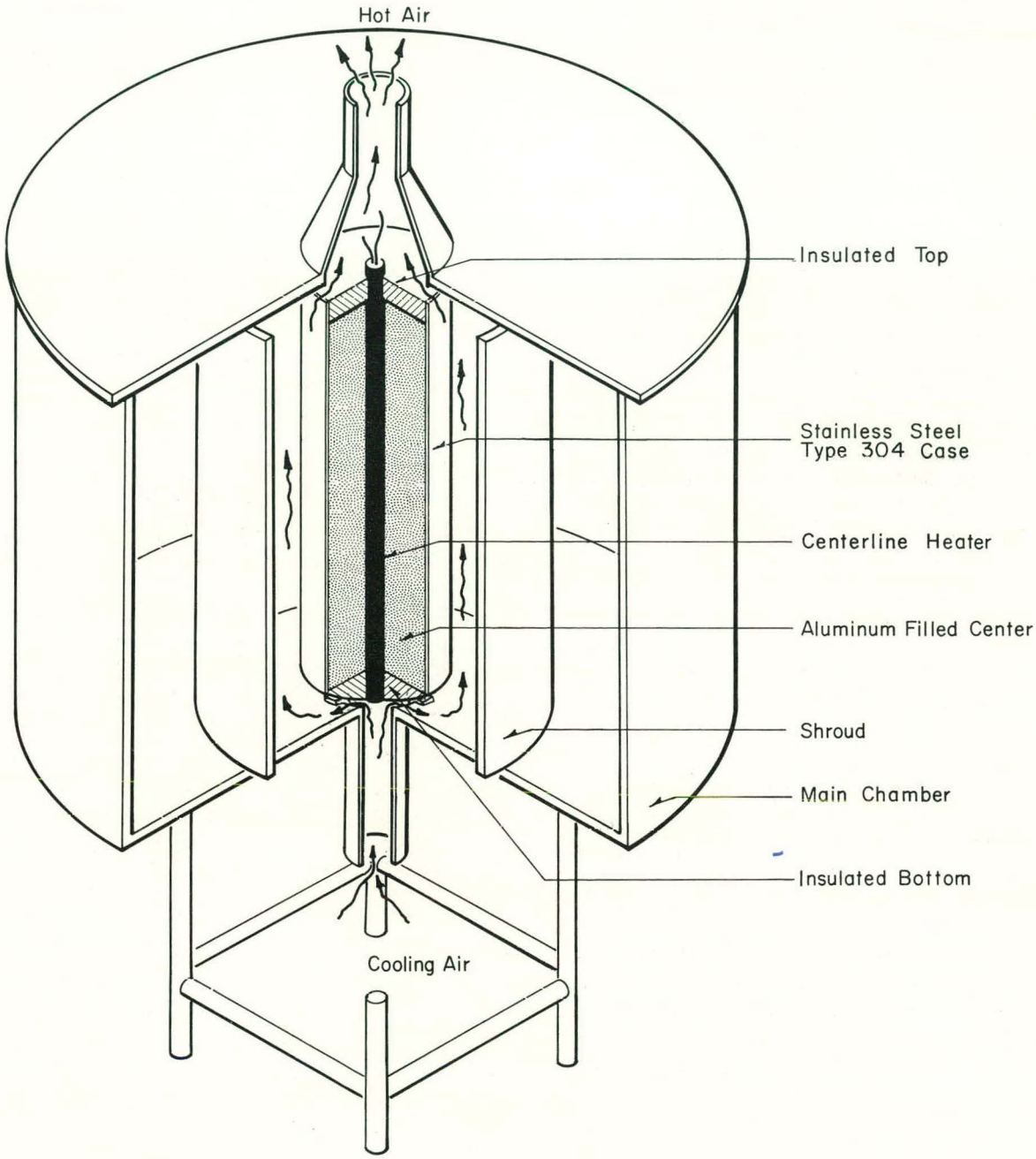

Figure 1. Experimental Equipment

"interference" fit. Before fitting the aluminum into the stainless steel pipe, the bottom weld cap was filled with insulation and the bottom electrical heater was inserted into the filler. After fitting the electrical heaters, the aluminum metal and the stainless steel case were forced together and the top of the unit was covered with insulation. This type of fabrication makes valid the assumption of uniform radial heat conduction implied in the analysis of the test results.

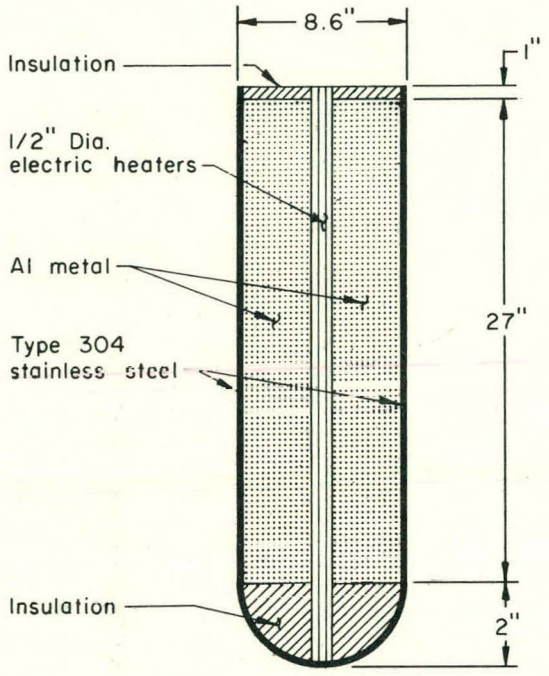

Figure 2. Cross-Section of Cylindrical Heat Source

Shrouds were fabricated of 1/8-inch thick sheets of Type 304 stainless steel. Shrouds with diameters of 9.3, 14.0, 20.6, and 32.6 inches were fabricated to provide annular spacings of 0.35, 2.7, 6, and 12-inches, respectively.

The source and one of the test shrouds were placed in the 48-inch-diameter chamber. Ports at the center of the bottom and top of the chamber provided channels for the inlet and outlet air flow, respectively. The top of the chamber was removable for changing shrouds. Iron-constantan thermocouples, connected to a common recorder, were spot-welded to the outside surface of the shell of the heat source and to the inside surface of the shroud at various angular and vertical positions as shown in Figure 3.

After electrical power was applied to the heaters, the temperatures of the source and the shroud were checked at hourly intervals until steady state was established. There were no hysteresis effects, and steady state temperatures were independent of the direction of power changes. The air was heated as it flowed upward through the annular space, and the air temperatures at the inlet and outlet were recorded. The room containing the apparatus was large enough to insure a constant air temperature at the inlet to the air space during a given test. However, the inlet air temperature did vary somewhat from day to day.

Since the emissivity of the stainless steel is quite sensitive to oxidation, the emissivity was calculated for the actual material

used. Inlet and outlet air temperatures and the air flow rate were measured for an air gap of 0.35 inches, and a heat balance across the air gap was used to calculate the emissivity of the stainless steel.

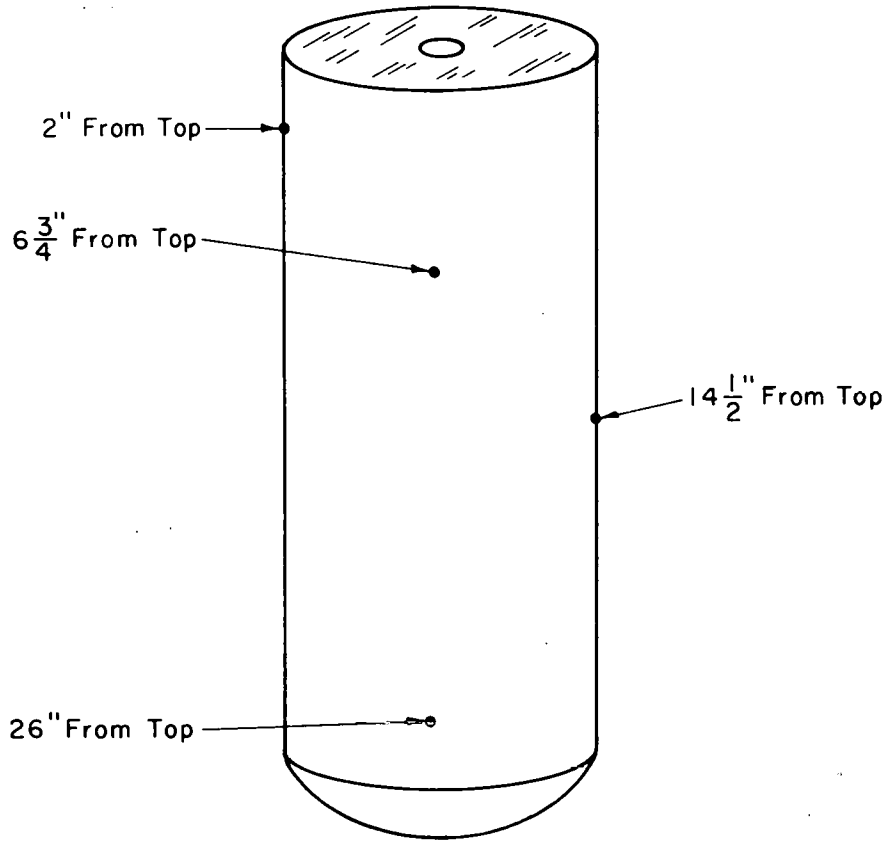

Figure 3. Location of Thermocouples on Cylindrical Heat Source.

III. DIFFERENTIATION BETWEEN RADIATIVE AND NATURAL CONVECTIVE HEAT TRANSFER RATES

Electrical power delivered to the centerline resistance heaters was dissipated from the surface of the cylindrical heat source by the mechanisms of radiation and natural convection. The total rate of heat dissipated from the surface of the source is given by:

$$Q_T = Q_R + Q_C \tag{5}$$

where:

Q_T = total rate of power supplied to the source, Btu/hr

Q_R = heat transferred by radiation, Btu/hr

Q_C = heat transferred by conduction and convection, Btu/hr.

The heat transferred by radiation from the surface of the source was calculated by the methods given in Appendix B. The rate at which heat was transferred by natural convection and conduction, Q_C, was calculated as the difference between the total power input, Q_T, and the calculated radiative heat transfer rate. A calibration of the wattmeter used in these tests showed a maximum deviation of ± five percent. A direct determination of the natural convective heat transfer rate from the source was not feasible because of the complex temperature gradients within the annulus.

Heat Transfer Rates

Calculation of the heat transferred by radiation from the source to the shroud was complicated by the temperature profile that existed along the length of the shroud (see Appendix A). Also, the radiative transfer through the open areas at the ends of the annulus becomes significant with increasing source-to-shroud spacings.

The formulae used to calculate the radiative heat transfer rates are presented and discussed in detail in Appendix B; only a summary of the methods used is presented here. For the smallest annular spacing, 0.35 inch, radiative transfer was calculated on the basis of infinite concentric cylinders[8]. This assumption permits neglecting the small areas at the ends of the annulus and results in a view factor (based on the area of the inner cylinder) of unity between the concentric cylinders. For the larger annular spaces, the area of the

annular ends was significant and the view factor from the inner to the outer cylinder was less than unity.

Radiative heat transfer rates for the 2.7-, 6-, and 12-inch annular spacings were calculated by the procedures outlined in Appendix B. The procedure given in Appendix B uses the absorption factor method reported by Gebhart[7]. The radiative heat transfer rates given in Table I are those calculated by approximating the temperature of the shroud by a series of constant temperature surfaces as presented in Appendix B.

Convective heat transfer rates from the inner cylinder, when heated without a shroud, were calculated using the simplified formula for heat transfer from vertical surfaces to air:

$$Q_c = h A (T_1 - T_a) \tag{6}$$

where:

A = area of inner cylinder, ft^2

T_1 = surface temperature of the cylinder, ^oF

T_a = ambient air temperature, ^oF

h = heat transfer coefficient, $Btu/hr\text{-}ft^2\text{-}^oF$.

The heat transfer coefficient was calculated by [6]:

$$h = 0.19 (T_1 - T_a)^{1/3} \tag{7}$$

Radiative heat transfer rates for the cylinder in an open room were determined by difference between the calculated convective rates and the total power delivered to the source. A heat source in a large room approximates the ideal case of a non-gray body radiating to black surroundings[6]. The radiant heat transfer rates determined by difference between the total heat input and the calculated natural convective heat transfer rates was used to determine the average emissivity of the source by the following relationships[6]:

$$Q_R = A_1 \varepsilon (1.5) (T_1^4 - T_a^4) \tag{8a}$$

where:

ε = emissivity of the source, dimensionless.

Table I

HEAT TRANSFER BALANCE AT THE SURFACE OF THE HEATED CYLINDER

Source-to-Shroud Annular Spacing (inches)	Total Heat Input, Q_T (Btu/hr)	Source Wall Temperature (°F)	Radiative Heat Transfer, Q_R (Btu/hr)	(%)	Natural Convective Heat Transfer, (Q_C) (Btu/hr)	(%)
0.35	170	120	49	29	121	71
	360	201	193	54	167	46
	680	209	285	41	395	59
	760	225	386	51	374	49
2.7	360	145	193	54	167	46
	760	210	480	63	280	37
	990	240	614	62	376	38
	1380	286	892	65	488	35
	1710	325	1173	69	537	31
	2210	370	1608	73	602	27
6	360	140	188	52	172	48
	550	175	334	61	216	39
	680	195	431	63	249	37
	1020	238	681	67	339	33
	1360	275	900	66	460	34
	1710	305	1130	66	580	34
12	170	110	96	56	74	44
	360	135	184	51	176	49
	680	181	418	61	262	39
	1090	220	657	60	433	40
	1360	245	840	62	520	38
	1710	275	1078	63	632	37
Heat Transfer without a Shroud	550	125	365	66	185	34
	1020	150	670	66	350	34
	1590	190	1020	64	570	36
	2390	240	1500	63	890	37
	3420	300	2130	63	1290	37

Emissivity of the stainless steel surfaces (shroud and heat source) was also determined from heat transfer measurements across the small air gap (0.35 inch). Measurements of the net air flow (by hot-wire anemometer) through the air gap and the inlet and outlet air temperatures were used to calculate the heat removed by natural convective flow. Tests were conducted at Rayleigh numbers less than 2000 to insure minimal radial convective heat transfer across the air gap. Radiative heat transfer rates were calculated by subtracting from the total power delivered to the heat source the heat removed by axial convective flow and that transferred by conduction across the air gap.

The following formula was used to calculate the emissivity of the stainless steel surfaces:

$$Q_R = \frac{\sigma (T_1^4 - T_2^4)}{\frac{1}{A_1\varepsilon_1} + \frac{1}{A_2}\left(\frac{1}{\varepsilon_2} - 1\right)} \qquad (8b)$$

where:

ε_1 (source emissivity) = ε_2 (shroud emissivity)

Data used in calculating the emissivities are shown in Table A-VI, Appendix A. The emissivities thus determined varied between 0.64 and 0.91, with an average of about 0.7 for five tests. This value for emissivity was used for all stainless steel surfaces when calculating radiative heat transfer rates (see Appendix B).

IV. DATA COMPARISON AND CORRELATION

Natural convective heat transfer from either cylindrical or flat vertical surfaces is widely discussed in the literature, and data correlations are given relating dimensionless Nusselt and Rayleigh numbers based on the height of the plate or cylinder[4,5,6,7]. Data from this study, when compared with the correlations presented for heat transfer from isolated surfaces, showed good agreement. This indicates that nearby surfaces have little effect on the mechanism of natural convective heat transfer.

An effective thermal conductivity across a fluid-filled annulus includes any effect of natural circulation within the annulus[4,5,6]. Heat transfer correlations are usually based on the temperature difference between the surfaces forming the enclosure. However, when the enclosure is open at the ends, as in this study, the fluid flowing through the annulus provides an additional heat sink. Data from this study are evaluated by calculating pseudo-effective thermal conductivities for annular spaces open at the ends and comparing with the effective thermal conductivities for enclosed spaces presented in the literature. The pseudo-effective thermal conductivities calculated herein are 1.2 - 1.8 times the effective thermal conductivities for equivalent enclosed spaces.

A correlation using modified Nusselt and Rayleigh numbers is presented using the temperature difference between the confining walls as a basis for the definition of the heat transfer coefficient. However, not all of the heat is transferred along a linear temperature gradient between the two surfaces because some heat is lost to the flowing air stream. Therefore, extrapolating this correlation beyond the limits of these tests may not be warranted.

1. Heat Transfer from Isolated and Shrouded Cylinders

The surface temperature of the heat source was essentially constant for a given power level; no attempt was made to measure the temperatures inside the aluminum-filled center. The variation of surface temperature of the source as a function of the reciprocal of the annular space is shown in Figure 4 for three typical heat fluxes. The independent variable (annular spacing) was plotted in reciprocal form so that data from tests without a shroud (limit of S as $S \to \infty$) could be included in Figure 4. At a given heat flux, the source wall temperature decreased with increasing source-to-shroud spacing, the temperature of the source being lowest when heated in the open room.

A comparison of the conventional data correlation for heat transfer from isolated cylinders with the data from this study is

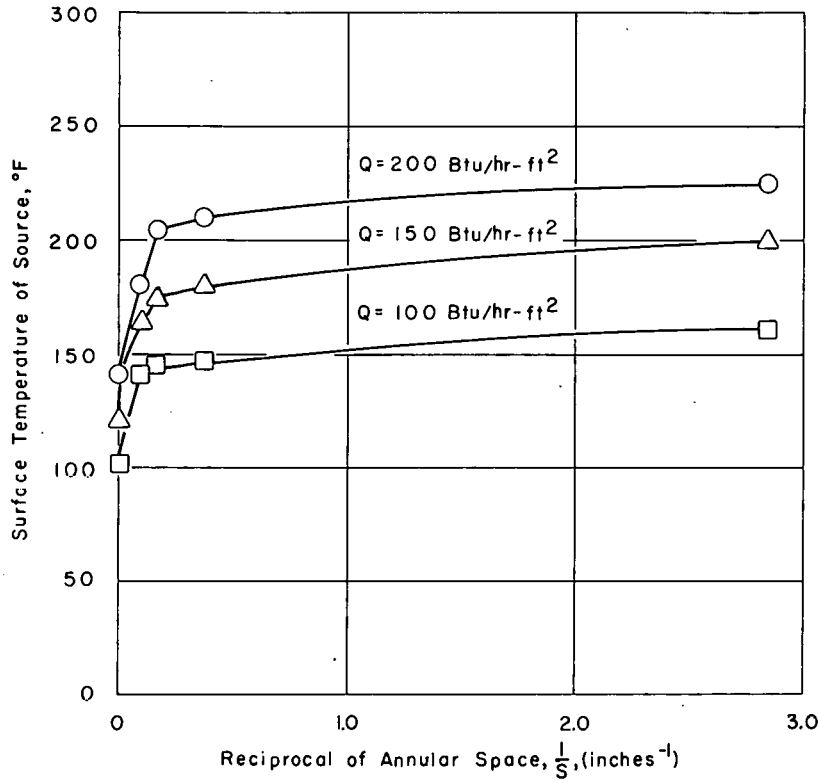

Figure 4. The Effect of Annular Space on the Temperature of the Source

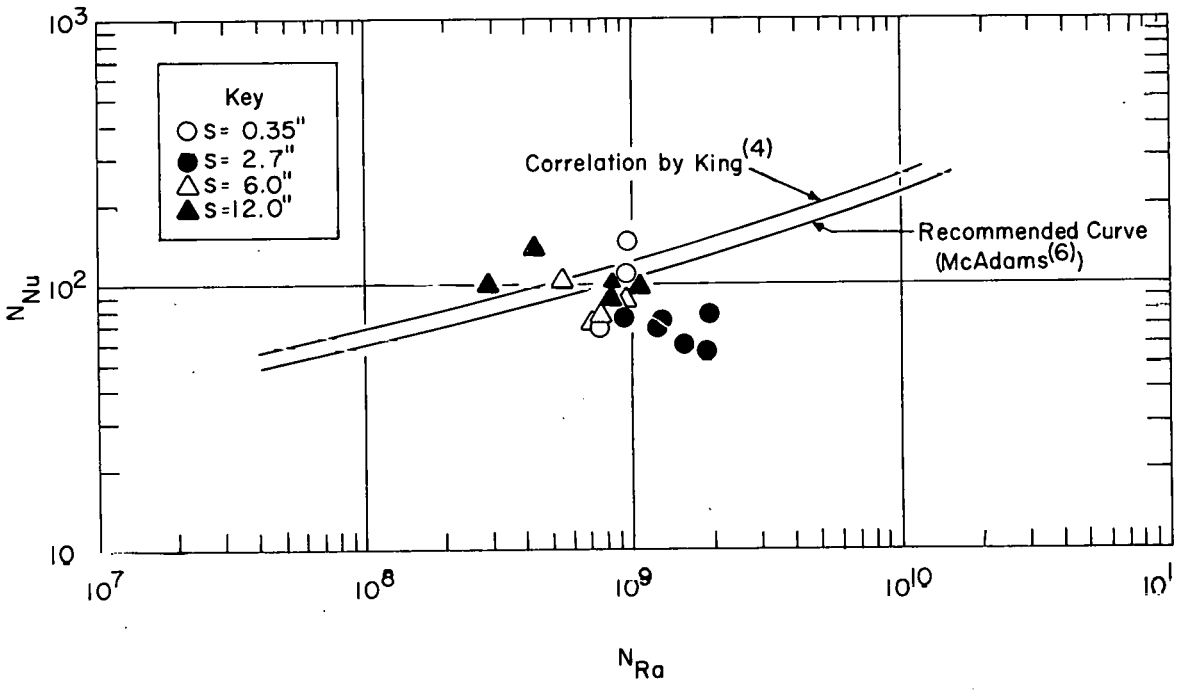

Figure 5. Heat Transfer from Isolated and Shrouded Vertical Surfaces

shown in Figure 5. No significant trends in data from this study are discernable; however, the presentation in Figure 5 does show that the correlations for heat transfer from isolated surfaces could be used to estimate heat transfer rates from shrouded surfaces. A factor that might contribute to the data scatter evident in Figure 5 is the fact that these tests were conducted near the laminar-to-turbulent transition region defined by a Rayleigh number of 10^9[6].

A more detailed study of the effect of nearby surfaces on natural convective heat transfer would require a knowledge of the temperature and air velocity variations within the annulus. The acquisition of these data was beyond the scope of this study. However, because radiation from nearby surfaces does result in higher temperatures of the gas and of the primary surface, the actual values of any heat transfer coefficients are increased slightly.

2. Annular Spaces with Ends Open or Closed

The data for heat transfer through annular spaces with closed or open ends is shown in Figure 6[5]. The correlation presented by Grober, Erk, and Grigull was developed for heat transfer through both vertical and horizontal annuli over a wide range of Prandtl numbers and annular spaces. The ratio of k_e/k determined in this study can be described by the following equation:

$$k_e/k = 0.27\,(N'_{Ra})^{0.25} \qquad (9)$$

The mechanisms of heat transfer within vertical annular spaces open at the ends is not completely analogous to heat transfer within enclosed annular spaces. At least part of the difference is the heat sink provided by the air stream flowing through the annulus when the annular ends are open.

At the point where the ratio (k_e/k) is unity ($\log_{10} k_e/k = 0$), it is assumed that no convective motion occurs and that all heat is transferred by simple conduction. A Rayleigh number of 1700 is considered as the limiting value for the start of free convection in completely enclosed annular spaces. For annular spaces open at both ends, convective motion in the annulus apparently starts at a Rayleigh number of about 100. For the case under study, a Rayleigh number of 1700 is obtained for an annular space of about 0.3 inch; a Rayleigh number of 100 is obtained for an annular space of about 0.1 inch.

Data from this study are compared in Figure 7 with the correlations by Jacob for heat transfer within enclosed spaces between parallel walls. Values of L/S reported by Jacob range from about 3 to 42. Values of L/S in this study ranged from 2.25 to 77. Data

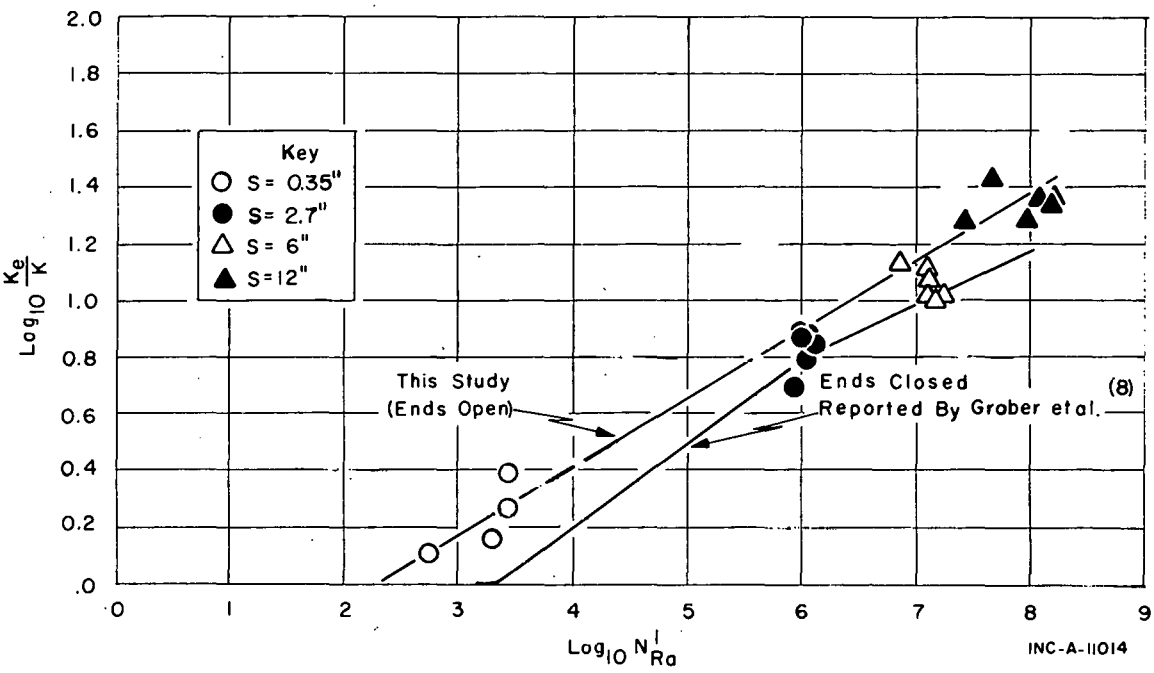

Figure 6. Comparison of Effective Thermal Conductivities Within Vertical Air-Filled Annuli

scatter prevented determining formulas similar to those given by Jacob. However, this comparison indicates that air circulating through an annulus increases the pseudo-effective thermal conductivity, especially at the smaller annular spacings.

The data scatter in this study, compared with Jacob's, may have been caused by the geometric and temperature differences. Data used by Jacob were obtained for heat transfer between parallel plates, both of which were at different but constant temperatures. Data for this study were obtained for heat transfer between concentric cylindrical surfaces where the temperature of the source was constant, but where the shroud temperature increased linearly with height.

3. Lorenz-Type Data Correlation

The data from this study can be correlated in the form originally proposed by Lorenz, as shown in Figure 8, where:

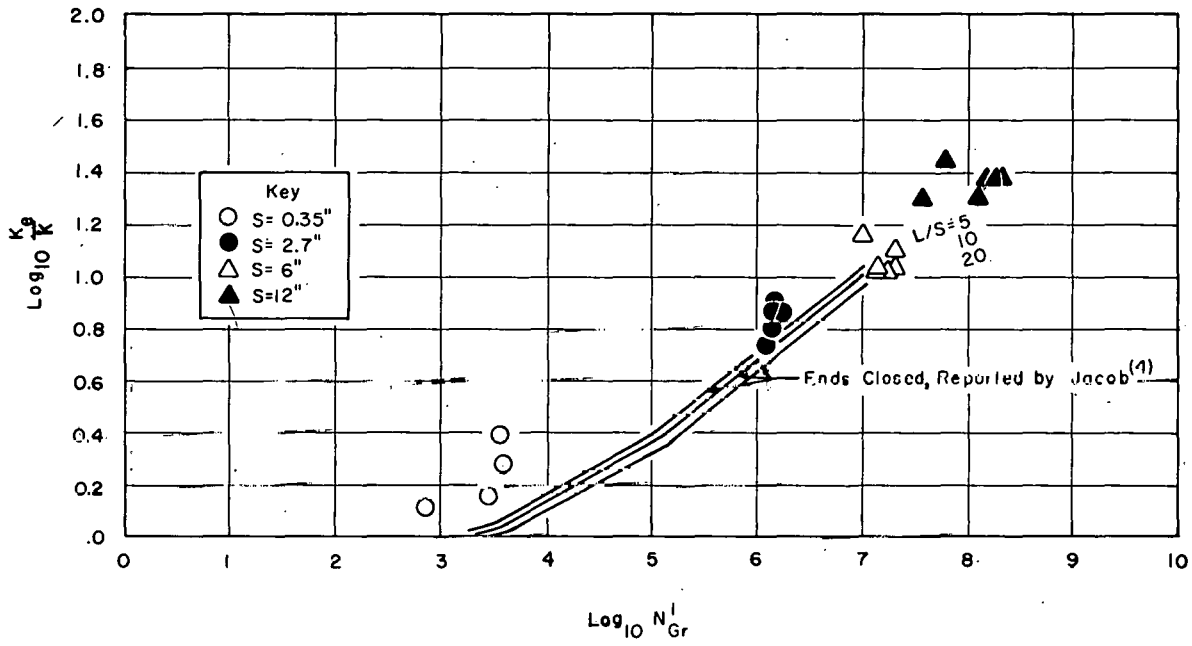

Figure 7. Comparison of Effective Thermal Conductivities Obtained in This Study with Those of Jacob[4]

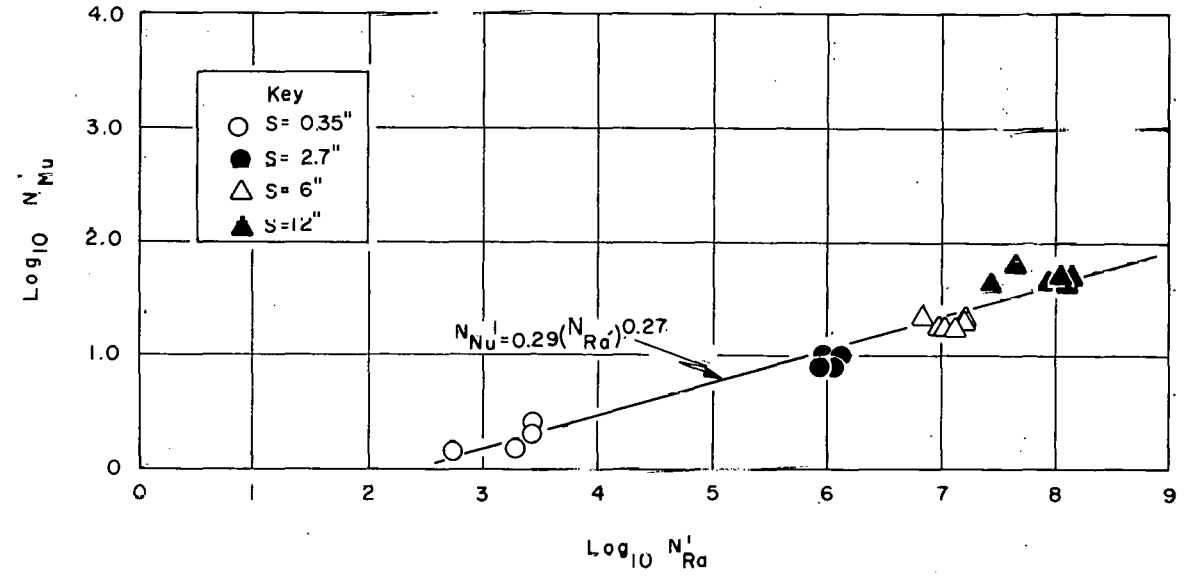

Figure 8. Lorenz-Type Correlation of Heat Transfer Within Vertical Air-Filled Annuli Open at the Ends

$$N'_{Nu} = 0.29\ (N'_{Ra})^{0.27} \tag{10}$$

and the modified Nusselt (N'_{Nu}) and Rayleigh (N'_{Ra}) numbers are based on the annular spacing.

The definition of the modified Nusselt number is:

$$N'_{Nu} = \frac{h_c S}{k} \tag{11}$$

where:

S = annular spacing, ft

k = thermal conductivity based on arithmetic mean temperature of the air, Btu/hr-ft-^{o}F

and h_c, the heat transfer coefficient, is defined by:

$$h_c = \frac{Q_c}{A_1\ (T_1 - \overline{T}_2)} \tag{12}$$

with

h_c = heat transfer coefficient, Btu/hr-ft^2-^{o}F

Q_c = convective heat transfer rate, Btu/hr

A_1 = area of inner cylinder, ft^2

T_1 = temperature of inner cylinder, ^{o}F

$\overline{T}_2$ = mean temperature of outer cylinder, ^{o}F

Application of both boundary layer theory and empirical methods has shown that the exponents of the Rayleigh number for laminar and turbulent flow are 1/4 and 1/3, respectively. Correlation of the data from this study by the method of Lorenz resulted in an exponent of 0.27, indicating that the flow was in the transition zone between laminar and turbulent flow. The conditions for the cessation of convective flow can be established as shown below; radiative heat transfer will be neglected.

At the point where convective motion ceases, heat transfer within the annulus is by conduction as given by the following equation:

$$q = \frac{k A_1 (T_1 - \bar{T}_2)}{S} \qquad (13)$$

For any Rayleigh number, the rate of heat transfer (by conduction and convection) is calculated by:

$$q = h_c A_1 (T_1 - \bar{T}_2) \qquad (14)$$

If there exists a Rayleigh number for which the modified Nusselt number ($N_{Nu} = h_c S/k$) equals one, then $h_c = k/S$. Substituting this value of h_c in Equation (14) yields Equation (13) which is for pure conduction. Thus, the necessary condition for convective motion to cease is $N_{Nu} = 1$.

Convective motion was observed to disappear at Rayleigh numbers below 100 for the vertical annulus with open ends; this compares with a Rayleigh number below 1700 quoted for a completely enclosed annulus[5].

V. CONCLUSIONS

The results of this study show that data for natural convective heat transfer from a shrouded, vertical cylinder agree reasonably well with the conventional Nusselt-Rayleigh number correlation for natural convective heat transfer from isolated vertical surfaces. Thus, the nearby surface (as close as 0.35 inch) did not significantly affect the mechanism of natural convective heat transfer. However, reflection of radiant energy from the shroud increased the temperature of the source and the air within the annulus over that for the case of an open source.

Heat transfer within the annular space was compared with the combination of natural convection and thermal conduction through an enclosed annular space. A pseudo-effective thermal conductivity, defined for an annulus open at the ends, was 1.2 - 1.8 times the effective thermal conductivity for an equivalent enclosed annulus. The increase in effective conductivity can be attributed to the heat transferred to the air flowing through the annulus. Thus, an annulus open at the ends offers less resistance to heat transfer than a corresponding enclosed annulus.

Data from this study were also correlated in terms of modified Nusselt and Rayleigh numbers.

Convective motion was observed to disappear at Rayleigh numbers below 100 for the vertical annulus with open ends; this compares with Rayleigh numbers below 1700 quoted for a completely enclosed annulus[5].

VI. NOMENCLATURE

A_1 = surface area of internally heated cylinder, ft^2

A_2 = surface area of concentric shroud, ft^2

A_3 = surface area of donut-shaped surface at top of annulus, ft^2

A_4 = surface area of donut-shaped surface at bottom of annulus, ft^2

A_{2_a} = elemental area on surface of concentric shroud, ft^2

A_{2_b} = elemental area on surface of concentric shroud, ft^2

A_{2_c} = elemental area on surface of concentric shroud, ft^2

A_{2_d} = elemental area on surface of concentric shroud, ft^2

A_{2_e} = elemental area on surface of concentric shroud, ft^2

a_{ik} = constant coefficient terms in simultaneous equations

B_{ik} = dimensionless absorption factor, fraction of radiant heat emitted from surface i and absorbed at surface k, dimensionless

F_{ik} = view factor from surface i to surface k, dimensionless

i,k = arbitrary subscripts referring to area A

g = local acceleration of gravity, ft/sec^2

h_c = natural convection heat transfer coefficient, $Btu/hr\text{-}ft^2\text{-}^oF$

K_i = $\varepsilon_i/1\text{-}\varepsilon_i$, dimensionless

L = vertical height, ft

N_{Pr} = Prandtl number

N'_{Gr} = Grashof number based on annular spacing as the characteristic length

N'_{Nu} = Nusselt number based on annular spacing as the characteristic length

N_{Nu} = Nusselt number based on height as the characteristic length

n = total number of surfaces, or exponents, depending on context

Q_c = heat transfer rate by natural convection, Btu/hr

Q_R = heat transfer rate by radiation, Btu/hr

Q_T = total heat transfer rate at surface of inner cylinder, Btu/hr

r = radius of internally heated cylinder, ft

N_{Ra} = Rayleigh number based on annular separation as the characteristic length

N_{Ra} = Rayleigh number based on height as the characteristic length

S = annular spacing between parallel surfaces, ft.

T = a surface temperature, ^{o}F

T_a = ambient temperature, ^{o}F

W_i = radiant heat flux from surface i, $Btu/hr\text{-}ft^2$

X = vertical plate height, feet or inches

Y = thickness of boundary layer, feet or inches.

GREEK SYMBOLS

α_{ik} = the quantity $F_{ik}\rho_k$, dimensionless

β = coefficient of thermal expansion, T^{-1}

Δ = an incremental change

ε = thermal emissivity of a surface, dimensionless

η = dimensionless width of velocity and temperature profile

μ = viscosity, $lb_m/ft\text{-}sec$

ρ = reflectivity, dimensionless

σ = Stefan-Boltzmann's constant, $Btu/ht\text{-}ft^2\text{-}^{o}R^4$

υ = kinematic viscosity, μ/ρ, ft^2/sec

VII. REFERENCES

1. B. R. Wheeler, et al, A Comparison of Various Calcination Processes for Processing High-Level Radioactive Wastes, USAEC Report No. IDO-14622, (April 1964).

2. D. E. Black and B. R. Dickey, Mathematical and Experimental Analysis of Heat Dissipation from Cylindrical Sources Buried in Soil, USAEC Report No. IN-1032, (December 1966).

3. J. R. Bower, Ed., Chemical and Process Development Branch Annual Report, Fiscal Year 1965, USAEC Report No. IDO-14661, (February 1966).

4. M. Jacob, Heat Transfer, Vol. I, John Wiley and Sons, Inc., New York, (1949).

5. H. Grober, S. Erk, and U. Grigull, Fundamentals of Heat Transfer, McGraw-Hill Book Company, New York, (1961).

6. W. H. McAdams, Heat Transmission, McGraw-Hill Book Co., Inc., New York, (1960).

7. B. Gebhart, Heat Transport, McGraw-Hill Book Co., New York, (1961).

8. R. B. Bird, et al, Transport Phenomena, John Wiley and Sons, Inc., New York, (1960).

9. F. Kreith, Radiation Heat Transfer for Spacecraft and Solar Power Plant Design, International Book Company, Scranton, Pa., (1962).

APPENDIX A

SUMMARY OF DATA

APPENDIX A

SUMMARY OF DATA

The data and calculations used in the body of the report are summarized herein. All of the data are given in terms of the source-to-shroud annular spacing and the total heat delivered to the heat source.

The linear temperature profile along the shroud is plotted in Figures A-1, A-2, A-3, and A-4. The designated points represent locations where the temperatures were measured. As shown by these figures, increasing the heat flux at the surface of the source increased the temperature gradient.

Temperatures of the various surfaces used in the calculations are given in Table A-I. The average temperature of the shroud and the temperatures of the five elemental areas are tabulated. The average temperature of the shroud is defined as the temperature at the vertical midpoint of the shroud. The temperatures of the elemental areas were determined by dividing the shroud into five equal segments and determining the temperature at the vertical midpoint of each segment.

The thermal emissivity used for stainless steel and carbon steel surfaces was 0.7 and 0.75, respectively[6]. The surface of the source and shroud was stainless steel Type 304; the enclosing chamber was carbon steel.

Areas used in the calculations are given in Table A-II.

The various dimensionless groups and parameters resulting from correlations given in the text are given in Table A-III. The physical constants for air were evaluated at the arithmetic average temperature of the inlet and outlet air.

Data used to prepare Figure 8 are tabulated in Table A-IV. Fluid properties were evaluated at a film temperature defined as the average temperature between the cylindrical source and the average air temperature in the vertical annular space. Nusselt and Rayleigh numbers were evaluated based on the height of the heated vertical cylinder. The heat transfer coefficients used in the Nusselt number were based on the temperature difference between the heated cylinder and the average air temperature in the annulus.

As indicated in the text, the emissivity of the source was determined by two separate tests. The shroud, also fabricated from Type 304 stainless steel, was assumed to have the same emissivity. Data for calculating the emissivity of the source and shroud is summarized in Tables A-V and A-VI.

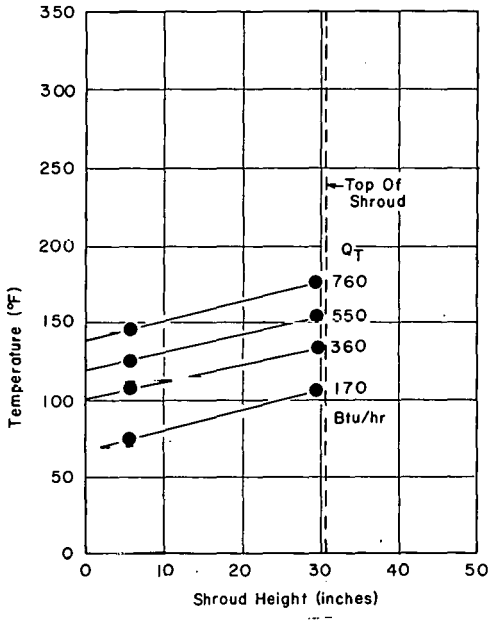

Figure A-1. Vertical Temperature Profile on Shroud at the 0.35-Inch Annular Separation.

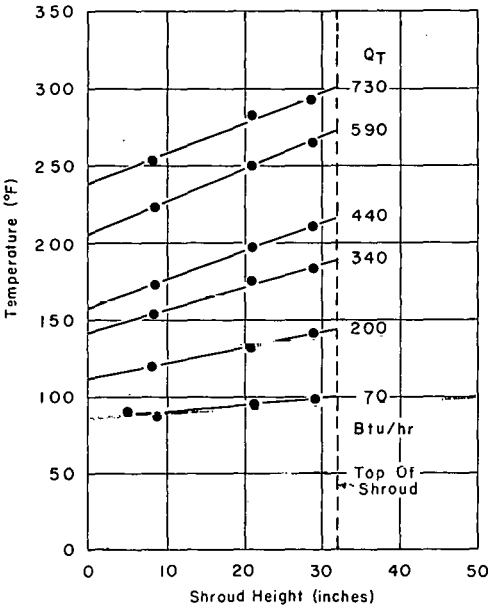

Figure A-2. Vertical Temperature Profile on Shroud at the 2.7-Inch Annular Separation

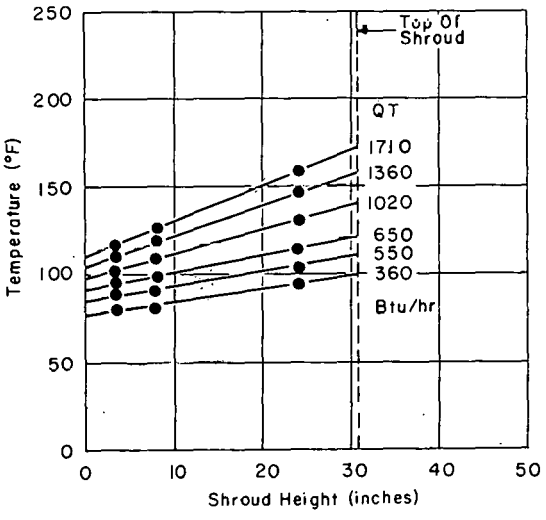

Figure A-3. Vertical Temperature Profile on Shroud at the 6-Inch Annular Separation

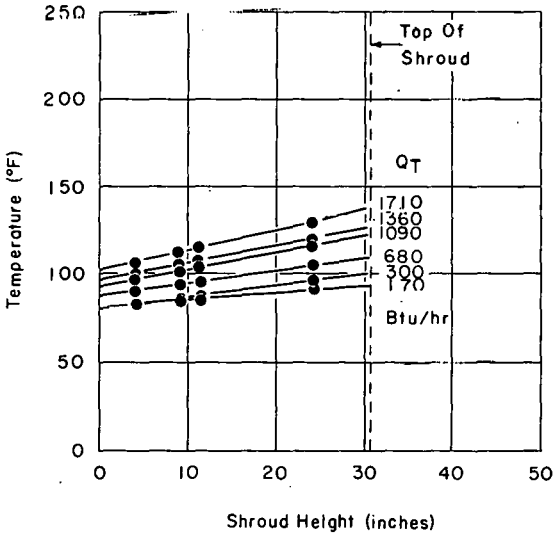

Figure A-4. Vertical Temperature Profile on Shroud at the 12-Inch Annular Separation

Table A-I

TEMPERATURES OF THE VARIOUS SURFACES

Source-to-Shroud Annular Spacing (inches)	Total Heat Input (Btu/hr)	Surface Temp. of Source (°F)	Average Temp. of Shroud (°F)	Average Temperature of Elemental Areas					Temp. of Annular Ends (°F)	Air Temp.	
				2a (°F)	2b (°F)	2c (°F)	2d (°F)	2e (°F)		In (°F)	Out (°F)
0.35	170	110	85	--	--	--	--	--	--	68	120
	360	170	125	--	--	--	--	--	--	82	125
	680	209	152	--	--	--	--	--	--	82	148
	760	225	153	--	--	--	--	--	--	88	154
2.7	360	145	93	90	92	95	97	100	68	69	90
	760	210	112	100	106	112	120	126	69	68	115
	990	240	128	120	125	130	135	140	70	68	131
	1380	286	149	134	142	150	158	166	75	68	151
	1710	325	166	150	160	170	175	180	80	68	170
	2210	370	190	170	180	190	200	210	80	68	190
6	360	140	90	80	85	90	94	98	68	76	112
	550	175	98	90	94	98	102	106	76	73	135
	680	195	103	95	99	103	106	110	79	79	154
	1020	238	113	105	109	113	117	121	82	78	176
	1360	275	132	120	126	132	138	144	85	82	186
	1710	305	141	125	133	141	149	157	87	82	204
12	170	110	87	85	86	87	88	89	80	80	98
	360	135	97	95	96	97	98	99	79	81	116
	680	181	102	100	101	102	103	104	82	88	117
	1090	220	110	102	105	110	113	116	82	82	136
	1360	245	113	105	109	113	117	121	80	74	144
	1710	275	118	110	114	118	122	126	85	76	184
No Shroud[a]	550	125	--	--	--	--	--	--	--	73	--
	1020	160	--	--	--	--	--	--	--	76	--
	1590	190	--	--	--	--	--	--	--	69	--
	2390	240	--	--	--	--	--	--	--	71	--
	3420	300	--	--	--	--	--	--	--	75	--

[a] Source was heated in an open room to provide a comparative basis. Air temperature given for these tests is the ambient temperature.

Table A-II

AREAS OF THE VARIOUS SURFACES

Source-to-Shroud Annular Spacing (inches)	Area of Source (ft^2)	Area of Shroud (ft^2)	Elemental Area[a] of Shroud (ft^2)	Area of Annulus (ft^2)
0.35	5.08	5.48	1.095	0.058
2.7	5.08	8.26	1.654	0.78
6	5.08	12.18	2.43	1.91
12	5.08	19.20	3.84	5.40

[a] The area of each elemental surface on the shroud is 1/5 of the total area.

The emissivity of carbon steel surfaces was assumed to be 0.75. No measurement was made of the emissivity of the carbon steel surfaces at the annular ends. The data used to calculate the emissivity of stainless steel, as explained in the text, is summarized in Table A-VI. Q_{flow} is the amount of heat dissipated by the free-flowing air stream.

Table A-III

PARAMETERS[a] USED IN DATA CORRELATIONS

Source-to-Shroud Annular Spacing (inches)	Total Heat Input (Btu/hr)	Grashof No. $N_{Gr'}$	Prandtl No. N_{Pr}	Rayleigh No. $N_{Ra'}$	k_e/k	h_c (Btu/hr-ft^2-$^\circ$F)	Modified Nusselt No.[a] $N_{Nu'}$
0.35	170	700	0.738	517	1.28	0.67	1.27
	360	2690	0.732	1970	1.48	0.77	1.43
	680	3600	0.732	2710	2.48	1.37	2.48
	760	3720	0.730	2710	1.89	1.04	1.88
2.7	360	13.0×10^5	0.742	9.7×10^5	7.70	0.67	9.9
	760	11.2×10^5	0.740	8.3×10^5	5.11	0.49	7.2
	990	14.0×10^5	0.738	10.3×10^5	7.50	0.52	9.6
	1380	15.7×10^5	0.736	11.4×10^5	6.16	0.55	7.7
	1710	13.9×10^5	0.735	10.0×10^5	7.45	0.68	9.5
	2210	17.6×10^5	0.734	12.9×10^5	7.12	0.67	9.2
6	360	9.8×10^6	0.735	7.2×10^6	13.9	0.68	22.2
	550	14.7×10^6	0.730	10.7×10^6	11.2	0.55	17.7
	680	14.3×10^6	0.728	10.4×10^6	10.5	0.53	16.5
	1020	19.2×10^6	0.725	13.9×10^6	10.3	0.53	16.3
	1360	23.2×10^6	0.720	16.7×10^6	12.0	0.63	19.0
	1710	23.2×10^6	0.718	16.8×10^6	12.9	0.69	20.5
12	170	3.7×10^7	0.740	2.7×10^7	19.8	0.61	41.0
	360	6.3×10^7	0.735	4.6×10^7	27.8	0.91	58.0
	680	13.0×10^7	0.730	9.5×10^7	19.9	0.66	42.0
	1090	16.7×10^7	0.728	12.1×10^7	23.5	0.77	48.7
	1360	20.7×10^7	0.725	15.0×10^7	23.2	0.78	48.8
	1710	20.2×10^7	0.720	14.5×10^7	23.0	0.79	48.2

[a] All terms are dimensionless except as noted.

Table A-IV

CONVENTIONAL NUSSELT AND RAYLEIGH NUMBERS

Source-to-Shroud Annular Spacing (inches)	Total Heat Input (Btu/hr)	$T_1-\bar{T}_{air}$ (^oF)	Rayleigh No. X (10^{-9})	Nusselt No.
0.35	170	8	0.12	---
	360	66	0.75	68
	680	94	0.96	110
	760	104	0.96	141
2.7	360	65	0.93	73
	760	98	1.29	72
	990	140	1.36	67
	1380	176	1.92	77
	1710	206	1.64	59
	2210	241	1.90	54
6	360	46	0.55	104
	550	71	0.73	83
	680	78	0.71	81
	1020	111	0.76	77
	1360	141	0.93	79
	1710	162	0.93	86
12	170	21	0.29	100
	360	36	0.43	135
	680	79	0.81	89
	1090	111	0.89	100
	1360	136	1.07	97
	1710	145	0.99	106
No Shroud	550	52	0.83	102
	1020	84	1.05	117
	1590	121	1.38	128
	2390	169	1.54	138
	3420	225	1.54	147

Table A-V

CALCULATED EMISSIVITY OF SOURCE IN OPEN ROOM

Total Heat Input (Btu/hr)	Radiant Heat Transfer Rate[a] (Btu/hr)	Temperature of the Source (°F)	Calculated Emissivity
550	365	125	0.76
1020	670	160	0.79
1590	1020	190	0.91
2390	1500	240	0.71
3420	2130	300	0.64

[a] Radiant heat transfer rate was the difference between total input rate and the calculated natural convective heat transfer rate.

Table A-VI

EMISSIVITIES BASED ON HEAT TRANSFER ACROSS 0.35-INCH GAP

Test	Heat Transfer Rates, Btu/hr				Calculated Emissivity
	Q_T	Q_{flow}	Q_{cond}	Q_R	
A	376	53	118	205	0.77
B	683	123	187	373	0.74
C	1025	170	269	586	0.73

APPENDIX B

DETERMINATION OF RADIATIVE HEAT TRANSFER RATES

APPENDIX B

DETERMINATION OF RADIATIVE HEAT TRANSFER RATES

The calculation of the net rate of heat transfer by radiation from each surface is described herein.

Assumptions basic to the methods developed below are:

1. Heat flux and temperature at the wall of the cylindrical heat source are constant.

2. The temperature of the shroud is a linear function of its height.

3. All surfaces are considered either grey or black.

4. The absorptivity of a surface is equal to its emissivity and independent of the source temperature of the incident radiation.

5. Radiation and reflection processes are diffuse.

Assumptions used in calculating the net radiative heat transfer from each surface are:

1. Concentric cylinders of infinite length (applies only for small air gaps).

2. A linear temperature profile on the surface of the shroud to determine an average temperature and calculate the net heat transferred by radiation between the source, shroud, and the two annular ends.

3. Approximation of the temperature on the surface of the shroud by the use of elemental areas, each at an average constant temperature.

B.1 Infinite Cylinders

The radiative heat transfer rates calculated by this method are based on constant temperatures on the surface of the shroud and inner cylinder. The following formula is available in the literature[8] for this case:

$$Q_R = \frac{\sigma (T_1^4 - \bar{T}_2^4)}{\frac{1}{A_1\varepsilon_1} + \frac{1}{A_2\varepsilon_2} - \frac{1}{A_2}} \qquad \text{(B-1)}$$

where:

the subscript 1 refers to the inner surface (source)

the subscript 2 refers to the outer surface (shroud)

$\overline{T}_2$ = mean temperature of the shroud.

Because this formula neglects the areas at the annular ends, it was used only for the 0.35-inch annular separation where the view factor between the two concentric surfaces was approximately unity. Results calculated from this formula are given in Table B-1

Table B-I

RADIATIVE HEAT TRANSFER RATES FROM SOURCE FOR 0.35-INCH ANNULAR SEPARATION

Total Heat Input[a] (Btu/hr)	Radiation Heat Transfer Rates (Btu/hr)
170	49
360	193
680	285
760	386

[a] Total heat input is the electrical power delivered to the cylinder source.

B.2 Absorption Factor Method

The absorption factor method[7] was used for both the four-surface and eight-surface cases. The derivation of the necessary equations will be followed by application to the data from the 2.7-, 6-, and 12-inch annular spacings using both the four-surface and the eight-surface cases.

The energy emitted from a grey surface within an enclosure of n surfaces can be represented by:

Rate at which energy is emitted by surface i = $A_i W_i$

where

$$W_i = \sigma \varepsilon_i T_i^4$$

A radiant heat balance between any surface j and the other surfaces yields

$$Q_j = W_jA_j - B_{1j}W_1A_1 - B_{2j}W_2A_2 - B_{jj}W_jA_j - \cdots - B_{nj}W_nA_n$$

$$= W_jA_j - \sum_{i=1}^{n} B_{ij}W_iA_i = W_jA_j(1-B_{jj}) - \sum_{\substack{i=1 \\ i\neq j}}^{n} B_{ij}W_iA_i \qquad \text{(B-2)}$$

where

Q_j = net radiant heat transfer rate from surface j, Btu/hr

A_j = area of surface j, ft^2

B_{ij} = absorption factor between surfaces i and j

W_i = radiative heat flux from surface i, Btu/hr-ft^2

The absorption factor B_{ij} is defined by

B_{ij} = total fraction of the energy emitted from surface i that is absorbed by surface j

Equation (B-2) has been written as above to emphasize the fact that the absorption factor for surface j is not necessarily zero, even for the case in which surface j does not "see" itself. Though a surface can "see" itself only when that surface is concave, the absorption factor B_{jj} can be greater than zero since some of the radiation emitted from j can be reabsorbed. Consider the absorption factor from surface 1 (the inner cylindrical heat source) to the general surface j

$$B_{1j} = \frac{\text{(total heat absorbed at surface j from 1)}}{\text{(total heat emitted from surface 1)}}$$

Then the rate at which heat is radiated from 1 and absorbed at j is given by

$$\text{Heat absorbed} = F_{1j}\varepsilon_jA_1W_1$$

where

F_{1j} = dimensionless view factor between surface 1 and j (see Appendix C)

ε_j = emissivity of surface j (see Appendix A, same as absorptivity)

The rate at which direct radiation from surface 1 is reflected at surface j is given by

Radiation from 1 reflected

$$= F_{1j}(1-\varepsilon_j)\, A_1 W_1 = F_{1j}\rho_j A_1 W_1$$

where the reflectivity ρ_j is given by:

$$1-\varepsilon_j = \rho_j$$

Since $F_{1i}\rho_i$ is reflected at the ith surface under conditions of diffuse radiation, the fraction of this indirect radiation absorbed at surface j is

$$\text{Indirect radiation absorbed at } j = F_{1i}\rho_i B_{ij}$$

The total fraction of heat absorbed at surface j from surface 1 can then be written as

$$B_{1j} = \left(F_{1j}\, j + \sum_{i=1}^{n} F_{1i}\rho_i B_{ij}\right) \tag{B-3}$$

For a system of n surfaces, n simultaneous equations each of the form of Equation (B-3) are obtained:

$$\begin{aligned}
B_{1j} &= F_{1j}\varepsilon_j + F_{11}\rho_1 B_{1j} + F_{12}\rho_2 B_{2j} + \ldots\ldots F_{1n}\rho_n B_{nj} \\
B_{2j} &= F_{2j}\varepsilon_j + F_{21}\rho_1 B_{1j} + F_{22}\rho_2 B_{2j} + \ldots\ldots F_{2n}\rho_n B_{nj} \\
&\ldots\ldots\ldots\ldots\ldots\ldots\ldots\ldots\ldots\ldots \\
B_{nj} &= F_{nj}\varepsilon_j + F_{n1}\rho_1 B_{1j} + F_{n2}\rho_2 B_{2j} + \ldots\ldots F_{nn}\rho_n B_{nj}
\end{aligned} \tag{B-4}$$

Equations B-4 can be rearranged and simplified by letting

$$F_{ik}\alpha_k = \alpha_{ik}$$

The system of equations can finally be written in the form

$$(\alpha_{11}-1)\, B_{1j} + \alpha_{12}B_{2j} + \alpha_{13}B_{3j} +\ldots+ \alpha_{1n}B_{nj} = -F_{1j}\varepsilon_j$$

$$\alpha_{21}B_{1j} + (\alpha_{22}-1)\, B_{2j} + \alpha_{23}B_{3j} +\ldots+ \alpha_{2n}B_{2n} = -F_{2j}\varepsilon_j \qquad \text{(B-5)}$$

$$\ldots\ldots\ldots\ldots\ldots\ldots\ldots\ldots\ldots\ldots$$

$$\alpha_{n1}B_{1j} + \alpha_{n2}B_{2j} + \alpha_{n3}B_{3j} +\ldots(\alpha_{nn}-1)\, B_{nj} = -F_{nj}\varepsilon_j$$

After the absorption factors are determined by solution of the set of simultaneous Equations (B-5), the net radiative heat transfer rate from any surface j may be calculated by Equation (B-2).

Equations (B-5) and (B-2) were solved on the IBM-7040 computer at the National Reactor Testing Station. The input data for the solution of these equations for the four-surface and eight-surface cases are shown in Tables B-II and B-III and in Tables B-IV and B-V respectively. The labels given in these tables refer to the areas designated in Figure B-1.

A short computer program, written for the IBM-7040, was also used to determine the radiative heat flux from each of the surfaces. The results are shown in Tables B-VI and B-VII for the four-surface and eight-surface cases, respectively. Net heat transferred from a surface is shown as a positive value, net heat transferred to a surface is shown as a negative value.

B.3 Comparison of Results

The eight-surface case is believed to be more accurate than the four-surface case because the linear temperature profile along the height of the shroud is taken into consideration. However, the differences in radiative heat transfer rates form the inner cylinder are not too great. The radiative heat transfer rates from the inner cylinder, calculated by both methods, are given in Table B-VIII.

Calculation of the radiative heat transfer rates could only have been calculated economically on a computer. For the 0.35-inch annular spacing of source to shroud, radiative heat transfer rates were determined by assuming that the cylinders were infinite in length. As the annular spacing is increased, the area at the ends of the annuli becomes a larger radiative heat sink. The results obtained for the eight-surface case most clearly show this effect by the fact that certain areas on the shroud emitted more radiant heat than they received from the source.

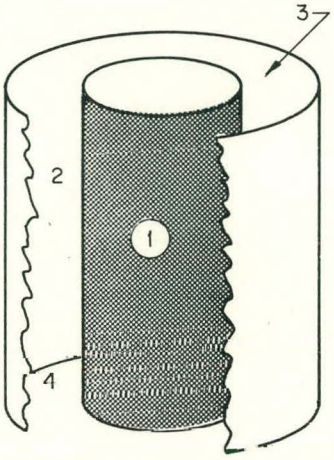

Four-Surface Case

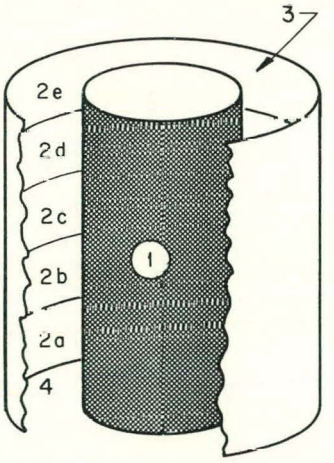

Eight-Surface Case

Fig. B-1. Areas Used for Determining the Radiative Heat Transfer Rates From the Surface of the Source

Table B-II

CONSTANT COEFFICIENTS FOR CALCULATION OF RADIATIVE HEAT TRANSFER RATES FOR THE FOUR-SURFACE CASE

Source-to-Shroud Annular Spacing	a_{ij} i	j = 1	2	3	4
2.7"	1	-1.000	.282	.008	.008
	2	.174	- .904[a]	.015	.015
	3	.054	.159	-1.000	.087
	4	.054	.159	.087	-1.000
6"	1	-1.000	.258	.021	.021
	2	.108	- .877[a]	.036	.036
	3	.054	.219	-1.000	.027
	4	.054	.219	.027	-1.000
12"	1	-1.000	.216	.042	.042
	2	.087	- .877[a]	.060	.060
	3	.039	.213	-1.000	.048
	4	.039	.213	.048	-1.000

[a] Note that a_{22} for all cases has a value greater than -1.000, since surface 2, the concave shroud, can "see" itself.

Table B-III

CONSTANT VECTORS FOR CALCULATION OF RADIATIVE HEAT TRANSFER RATES FOR THE FOUR-SURFACE CASE

Source-to-Shroud Annular Spacing	$F_{ij}\epsilon_j$ i	j = 1	2	3	4
2.7"	1	0	.406	.126	.126
	2	.650	.224	.371	.371
	3	.0196	.035	0	.203
	4	.0196	.035	.203	0
6"	1	0	.252	.126	.126
	2	.602	.287	.511	.511
	3	.049	.084	0	.063
	4	.049	.084	.063	0
12"	1	0	.133	.091	.091
	2	.504	.287	.497	.497
	3	.098	.140	0	.112
	4	.098	.140	.112	0

Table B-IV

CONSTANT COEFFICIENTS FOR CALCULATION OF RADIATIVE HEAT TRANSFER RATES FOR THE EIGHT-SURFACE CASE

Source-to-Shroud Annular Spacing	a_{ij} i	j 1	2a	2b	2c	2d	2e	3	4
2.7"	1	-1.000	.051	.057	.060	.057	.050	.008	.008
	2a	.165	- .946	.033	0	0	0	0	.048
	2b	.180	.033	- .946	.033	0	0	0	0
	2c	.180	0	.033	- .946	.033	0	0	0
	2d	.180	0	0	.033	- .946	.033	0	0
	2e	.165	0	0	0	.033	- .946	.048	0
	3	.054	0	0	0	.057	.102	-1.000	.087
	4	.054	.102	.057	0	0	0	.087	-1.000
6"	1	-1.000	.042	.051	.072	.051	.042	.021	.021
	2a	.096	- .955	.030	.006	0	0	0	.105
	2b	.126	.030	- .955	.020	.006	0	.012	.063
	2c	.150	.006	.030	- .955	.030	.006	.015	.015
	2d	.126	0	.006	0.03	- .955	.03	.063	.012
	2e	.096	0	0	.006	.03	- .955	.105	0
	3	.054	0	.015	.017	.048	.132	-1.000	.027
	4	.054	.132	.048	.027	.015	0	.027	-1.000
12"	1	-1.000	.039	.045	.048	.045	.039	.042	.042
	2a	.054	- .961	.033	.015	.003	0	.006	.144
	2b	.060	.033	- .961	.033	.015	.003	.012	.105
	2c	.063	.015	.033	- .961	.033	.015	.051	.051
	2d	.060	.003	.015	.033	- .961	.033	.105	.012
	2e	.054	0	.003	.015	.033	- .961	.144	.006
	3	.039	0	.009	.036	.075	.102	-1.000	.048
	4	.039	.102	.075	.036	.009	0	.048	-1.000

Table B-V

CONSTANT VECTORS FOR CALCULATION OF RADIATIVE HEAT TRANSFER RATES FOR THE EIGHT-SURFACE CASE

Source-to-Shroud Annular Spacing	$F_{ij}\varepsilon_j$ i \ j	1	2a	2b	2c	2d	2e	3	4
2.7"	1	0	.385	.420	.420	.420	.385	.126	.126
	2a	.119	.126	.077	0	0	0	0	.128
	2b	.133	.077	.126	.077	0	0	0	.133
	2c	.140	0	.077	.126	.077	0	0	0
	2d	.133	0	0	.077	.126	.077	.126	0
	2e	.119	0	0	0	.077	.126	.128	0
	3	.0196	0	0	0	0	.048	0	.204
	4	.0196	.048	0	0	0	0	.204	0
6"	1	0	.224	.294	.350	.294	.224	.126	.126
	2a	.098	.105	.070	.014	0	0	0	.308
	2b	.119	.070	.105	.070	.014	0	.035	.112
	2c	.168	.014	.070	.015	.070	.014	.063	.063
	2d	.119	0	.014	.070	.105	.070	.112	.035
	2e	.098	0	0	.014	.070	.015	.308	0
	3	.049	0	.018	.035	.147	.245	0	.063
	4	.049	.245	.147	.035	.028	0	.063	0
12"	1	0	.126	.140	.147	.140	.126	.091	.091
	2a	.091	.091	.077	.035	.007	0	0	.238
	2b	.105	.077	.091	.077	.035	.007	.021	.175
	2c	.112	.035	.077	.091	.077	.035	.084	.084
	2d	.105	.007	.035	.077	.091	.077	.175	.021
	2e	.091	0	.007	.035	.077	.091	.238	0
	3	.098	.024	.028	.119	.235	.336	0	.112
	4	.098	.336	.235	.119	.028	.014	.112	0

Table B-VI

RADIATIVE HEAT TRANSFER RATES FROM ALL SURFACES
DETERMINED FOR THE FOUR-SURFACE CASE

Source-to-Shroud Annular Spacing	Total Heat Input[a] (Btu/hr)	Radiative Heat Transfer Rates (Btu/hr)			
		1	2	3	4
2.7"	360	220	- 178	- 21	- 21
	990	650	- 538	- 56	- 56
	1710	1215	-1017	- 99	- 99
	2210	1599	-1318	-140	-140
	3010	2572	-2157	-207	-207
	3720	3426	-2876	-275	-275
6"	360	244	- 147	- 49	- 49
	550	379	- 239	- 70	- 70
	680	474	- 304	- 85	- 85
	1020	723	- 478	-123	-123
	1390	976	- 652	-162	-162
	1710	1221	- 828	-196	-196
12"	170	119	- 57	- 31	- 31
	360	232	- 123	- 55	- 55
	680	441	- 188	-127	-127
	1020	691	- 333	-179	-179
	1380	877	- 429	-223	-223
	1710	1107	- 562	-273	-273

(a) Total rate of heat input is the electrical power delivered to the cylindrical source.

Table B-VII

RADIATIVE HEAT TRANSFER RATES FROM ALL SURFACES
DETERMINED FOR THE EIGHT-SURFACE CASE

Source-to-Shroud Annular Spacing	Total Heat Input (Btu/hr)[a]	Radiative Heat Transfer Rates (Btu/hr)							
		1	2a	2b	2c	2d	2e	3	4
2.7"	360	193	- 35	- 59	- 50	- 54	- 24	- 15	- 15
	760	480	- 59	-105	-110	-119	- 90	- 2	- 1
	990	614	-107	-144	-136	-133	- 81	- 74	- 61
	1380	892	-112	-182	-194	-201	-158	- 21	- 12
	1710	1173	-207	-258	-246	-238	-161	- 33	- 30
	2210	1608	-281	-348	-340	-318	-212	- 56	- 52
6"	360	188	- 48	- 44	- 30	- 24	- 10	- 68	- 52
	550	334	- 72	- 26	- 60	+ 5	- 29	- 84	- 68
	680	431	- 89	- 40	- 79	- 7	- 40	- 96	- 80
	1020	681	-130	- 76	-126	- 37	- 67	-131	-113
	1380	900	-168	-104	-163	- 52	- 76	-183	-156
	1710	1130	-213	-140	-207	- 75	- 92	-222	-185
12"	170	96	- 13	- 8	- 6	- 4	+ 23	- 60	- 55
	360	184	+ 19	- 7	- 7	- 3	+ 29	-111	-105
	680	413	- 6	- 38	- 40	- 33	+ 4	-156	-150
	1020	657	- 39	- 71	- 64	- 50	- 32	-228	-205
	1380	840	- 55	- 88	- 87	- 68	-100	-278	-253
	1710	1073	- 84	-121	-122	-101	- 37	-319	-294

(a) Total rate of heat input is the electrical power delivered to the cylindrical source.

Table B-VIII

SUMMARY OF RADIATIVE HEAT TRANSFER RATES

Source-to-Shroud Annular Spacing (inches)	Total Heat Input[a] (Btu/hr)	Total Radiative Heat Transfer Rates From the Source Using: Four-Surface Case (Btu/hr)	Eight-Surface Case (Btu/hr)
2.7	360	220	193
	990	650	614
	1710	1215	1173
	2210	1599	1608
	3010	2572	2491
	3720	3426	3350
6	360	244	188
	550	379	334
	680	474	431
	1020	723	681
	1380	976	900
	1710	1221	1130
12	170	119	96
	360	232	184
	680	441	418
	1020	691	657
	1380	877	840
	1710	1107	1078

(a) Total rate of heat input is the electrical power delivered to the cylindrical source.

APPENDIX C

VIEW FACTOR DETERMINATION

APPENDIX C

VIEW FACTOR DETERMINATION

View factors between the various surfaces form an integral part of the solution for radiative heat transfer rates. Shape factor curves, available in the literature[9], and view factor algebra were used to calculate the various view factors given in this appendix for the 2.7-, 6-, and 12-inch annular spacings.

1. View Factors for the Four-Surface Case

View factors between the surfaces in the four-surface case are given in Tables C-I, C-II, and C-III. The surfaces represented by numbers in the tables and shown in Figure C-1 are defined by the following: Surface 1 -- heat source, or cylinder; Surface 2 -- shroud, or outer cylinder; Surface 3 -- top of vertical annulus; and Surface 4 -- bottom of vertical annulus.

The view factors, F_{21} and F_{22}, were obtained directly from published view factor curves[9]. Algebraic manipulation by basic view factor algebra and the use of the symmetrical geometry of the system were used to obtain the other view factors.

View factors between various surfaces as a function of the annular spacing are shown in Figure C-2. The view factor F_{12} represents that fraction of the outer cylinder "seen" by the inner cylinder, which decreases as the annular spacing increases. That fraction of the ends of the annulus "seen" by the surface 1, F_{13} or F_{14}, increases with increasing annular spacing. The view factor F_{22}, representing the fraction that the outer cylinder "sees" of itself, passes through a maximum with increasing annular spacing.

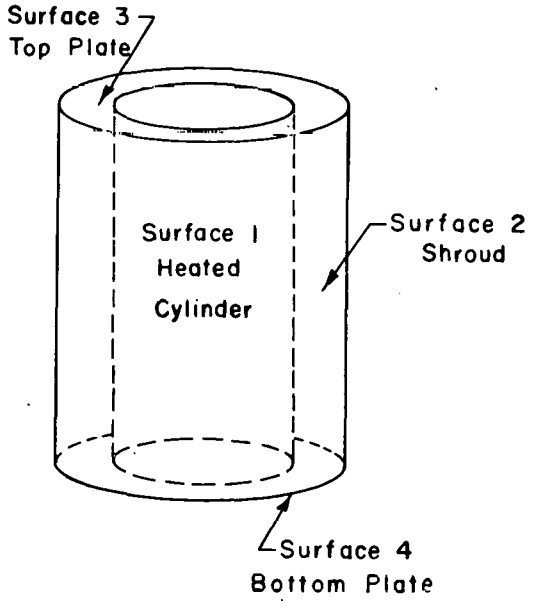

Figure C-1. Surfaces Used for Four-Surface Solution of Radiative Heat Transfer Rates

2. View Factors for the Eight-Surface Case

As mentioned earlier, the radiative heat transfer formulas were

TABLE C-I

VIEW FACTORS FOR 2.7-INCH ANNULAR SPACE IN THE FOUR-SURFACE CASE

F_{ij}	Surface j			
	1	2	3	4
Surface i 1	---	.94	.028	.028
2	0.58	0.32	0.05	0.05
3	0.18	.53	---	.29
4	0.18	.53	.29	---

TABLE C-II

VIEW FACTORS FOR 6-INCH ANNULAR SPACE IN THE FOUR-SURFACE CASE

F_{ij}	Surface j			
	1	2	3	4
Surface i 1	---	0.86	0.07	0.07
2	0.36	0.41	0.12	0.12
3	.18	.73	---	0.09
4	.18	.73	0.09	---

TABLE C-III

VIEW FACTORS FOR 12-INCH ANNULAR SPACE IN THE FOUR-SURFACE CASE

F_{ij}	Surface j			
	1	2	3	4
Surface i 1	---	0.72	0.14	0.14
2	0.19	0.41	.20	.20
3	.13	.71	---	0.16
4	.13	.71	0.16	---

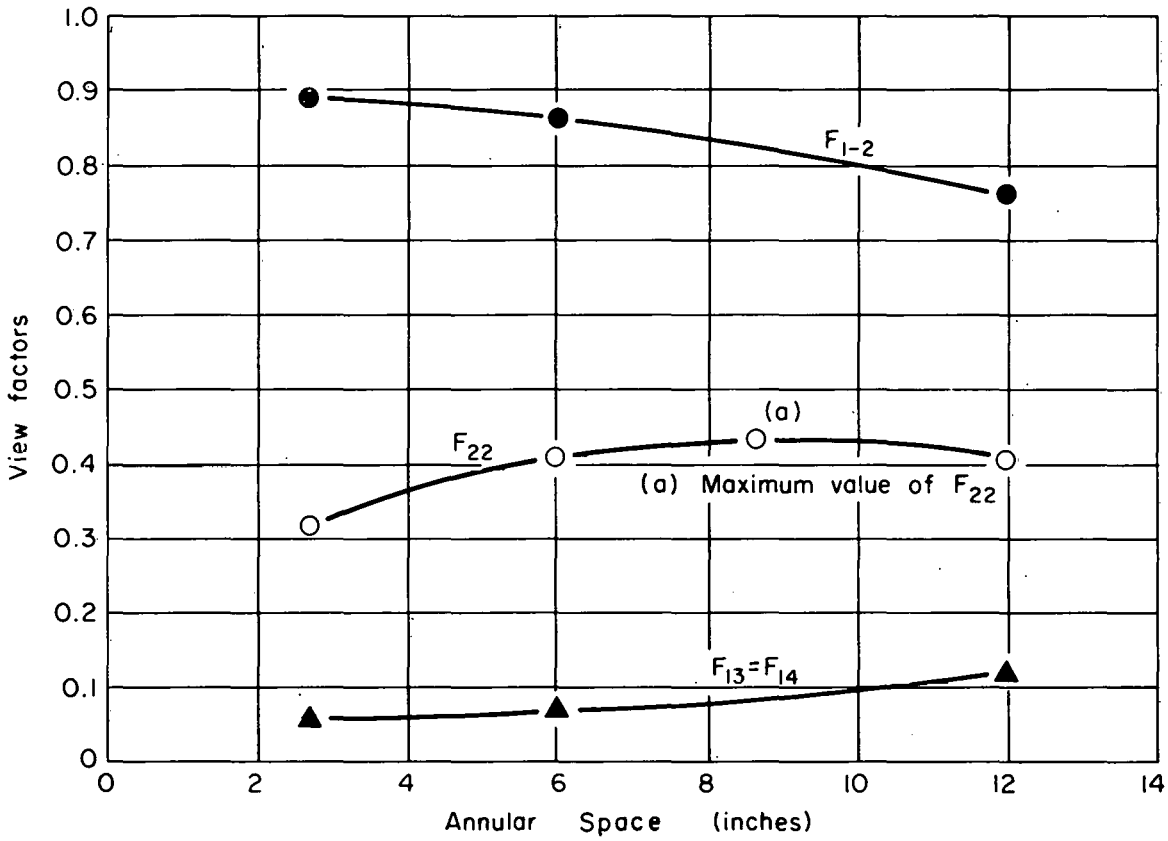

Figure C-2. Effect of Annular Separation on View Factors for Four-Surface Case

derived for this case by dividing the area of the shroud into five equal elemental areas, each at a constant temperature. View factors used in the eight-surface case are given in Tables C-IV through C-VI. The five elemental areas on the shroud are designated 2a through 2e as shown in Figure C-3. As shown in Tables C-IV through C-VI, the elemental areas on the shroud could "see" themselves as well as neighboring elemental areas in addition to the source and the annular ends.

Some values of the various view factors appear repeatedly because of the symmetry of the system. The view factors from surface 1 to the ends and from each end to surface 1 are identical in both the four- and eight-surface cases. The sum of the view factors from the inner cylinder to each elemental area on the surface of the shroud must equal the view factor between the inner cylinder and the entire shroud within the accuracy of values read from the shape factor curves.

The effect of annular spacing on the view factors from the heat source (surface 1) are graphically shown in Figure C-4. As expected,

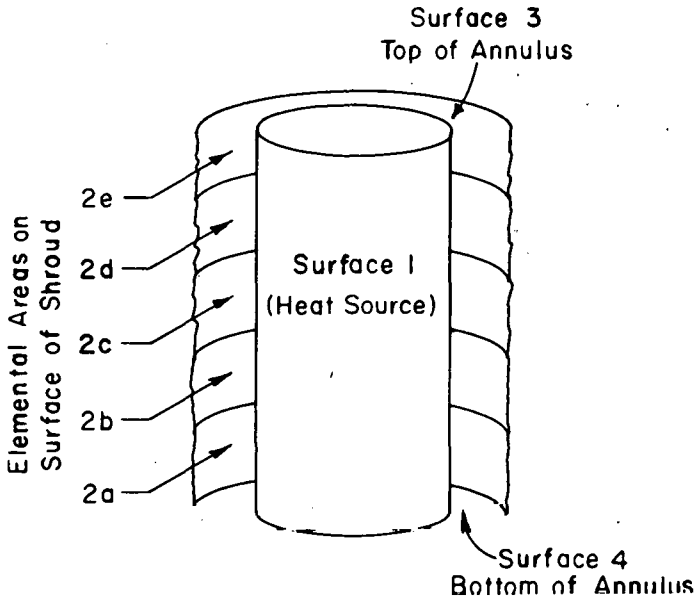

Fig. C-3. Surfaces Used for Eight-Surface Solution of Radiative Heat Transfer Rates.

Table C-IV

VIEW FACTORS FOR 2.7-INCH ANNULAR SPACE IN THE EIGHT-SURFACE CASE

F	1	2a	2b	2c	2d	2e	3	4
1	--	.17	.19	.20	.19	.17	0.028	0.028
2a	0.55	0.18	0.11	0	0	0	0	0.16
2b	.60	0.11	0.18	0.11	0	0	0	0
2c	.60	0	0.11	0.18	0.11	0	0	0
2d	0.60	0	0	0.11	0.18	0.11	0	0
2e	0.55	0	0	0	0.11	0.18	0.16	0
3	0.18	0	0	0	0.19	0.34	--	0.29
4	0.18	0.34	0.19	0	0	0	0.29	--

Table C-V

VIEW FACTORS FOR 6-INCH ANNULAR SPACE
IN THE EIGHT-SURFACE CASE

F_{ij}	1	2a	2b	2c	2d	2e	3	4
1	--	0.14	0.17	0.24	0.17	0.14	0.07	0.07
2a	0.32	0.15	0.10	0.02	0	0	0	0.35
2b	0.42	0.10	0.15	0.10	0.02	0	0.04	0.21
2c	0.50	0.02	0.10	0.15	0.10	0.02	0.05	0.05
2d	0.42	0	0.02	0.10	0.15	0.10	0.21	0.04
2e	0.32	0	0	0.02	0.10	0.15	0.35	0
3	0.18	0	0.05	0.09	0.16	0.44	0	0.09
4	0.18	0.44	0.16	0.09	0.05	0	0.09	0

Table C-VI

VIEW FACTORS FOR 12-INCH ANNULAR SPACE
IN THE EIGHT-SURFACE CASE

F_{ij}	1	2a	2b	2c	2d	2e	3	4
1	--	0.13	0.15	0.16	0.15	0.13	0.14	0.14
2a	0.18	0.13	0.11	0.05	0.01	0	0.02	0.48
2b	0.20	0.11	0.13	0.11	0.05	0.01	0.04	0.35
2c	0.21	0.05	0.11	0.13	0.11	0.05	0.17	0.17
2d	0.20	0.01	0.05	0.11	0.13	0.11	0.35	0.04
2e	0.18	0	0.01	0.05	0.11	0.13	0.48	0.02
3	0.13	0	0.03	0.12	0.25	0.34	--	0.16
4	0.13	0.34	0.25	0.12	0.03	0	0.16	--

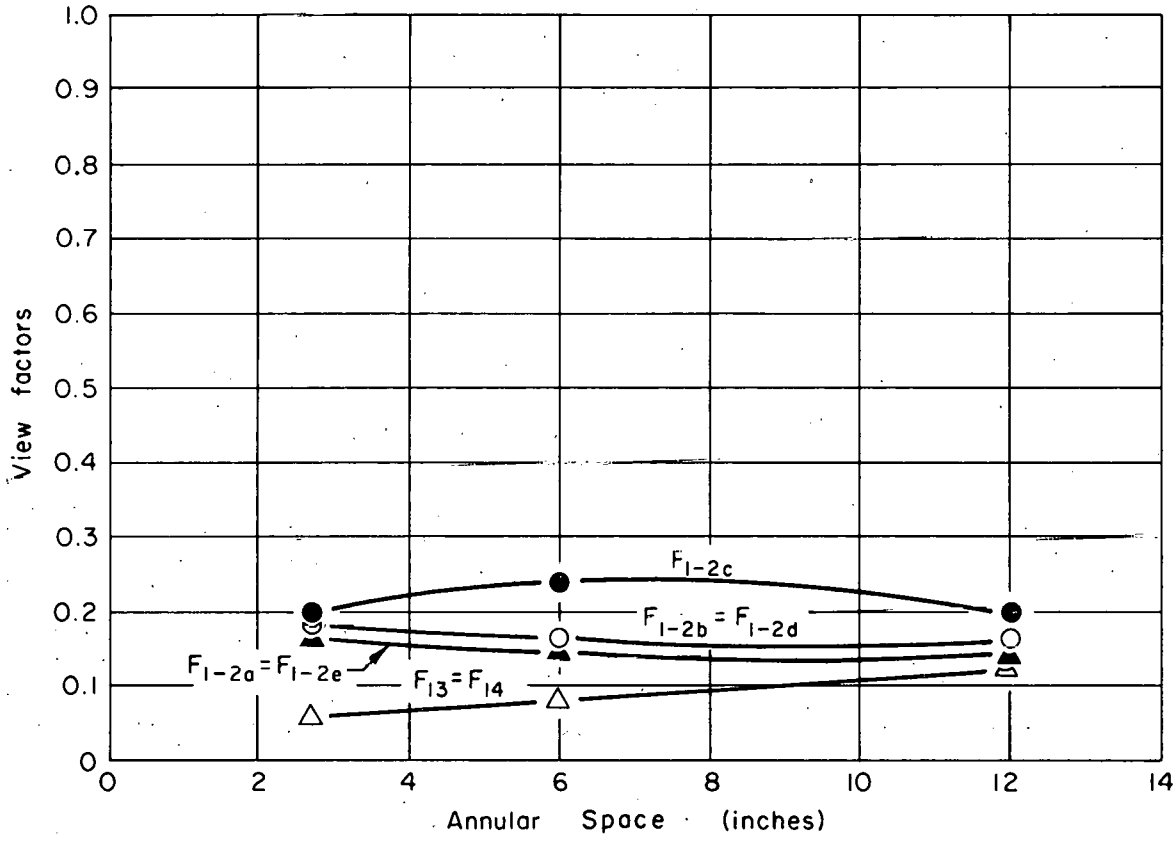

Figure C-4. View Factors for Eight-Surface Solution As Affected by Annular Separation

the view factors from surface 1 to the elemental areas on the shroud, surface 2, decrease with an increase in the annular spacing.

As in the earlier case, algebraic manipulation and use of symmetry were used to determine many of the view factors for the eight-surface case. The complexity in calculating the view factors increases rapidly with the number of surfaces. Since the accuracy of view factors generally decreases as the number of surfaces increases, the approximation of a large surface by a number of smaller surfaces is justified only if the temperature of the large surface varies significantly.